COMPARISON OF LIBS AND POLARIZATION RESOLVED LIBS EMISSION SPECTRA FOR ALUMINIUM ALLOY**

G. A. Wubetu [1,2*], J. T. Costello [3], T. J. Kelly [4], P. Wachulak [5], A. Bartnik [5], W. Skrzeczanowski [5], H. Fiedorowicz [5]

[1] Department of Physics, College of Science at Bahir Dar University Bahir Dar, Ethiopia; e-mail: getasew.wubetu2@mail.dcu.ie, getasew.admasu@bdu.edu.et
[2] Department of Physics, College of Natural and Computational Science at Addis Ababa University, Addis Ababa, Ethiopia
[3] National Centre for Plasmas Science and Technology (NCPST) and School of Physical Science at Dublin City University, Glasnevin, Dublin, Ireland
[4] Department of Computer Science and Applied Physics, Atlantic Technological University, Galway, Ireland
[5] Institute of Optoelectronics, Military University of Technology (MUT), Warsaw, Poland

Time and polarization resolved optical emission spectroscopy of laser-produced plasmas formed on Al alloys has been studied in the visible spectral range at a background air pressure of 10^{-4} mbar. A comparative experimental investigation has been made between the results obtained from the polarization-resolved laser-induced breakdown spectroscopy (PRLIBS) and those obtained for the unresolved case (denoted simply as LIBS here). The spectral signal-to-background ratio (SBR) is increased significantly for PRLIBS compared with LIBS for the Mn emission line at a wavelength of 415 nm, which had trace concentrations in the sample. The results have been interpreted within the framework of radiatively recombining plasma where free electrons are captured by ions to emit radiation. In addition, the degree of polarization is quantified for two matrix lines, namely Al^0 (at 396.15 nm) and Al^{2+} (569.6 nm) by using neighbouring unpolarised emission lines. The plasma parameters are measured and compared with the degree of polarization to determine the dominant mechanism for the polarised emission. Thus, from these results, we feel confident that PRLIBS is a useful and simple addition, capable of improving experimental LIBS performance.

Keywords: *laser-induced breakdown spectroscopy, polarization-resolved laser-induced breakdown spectroscopy, signal-to-background ratio, limit of detection, radiative recombination.*

СРАВНЕНИЕ ВРЕМЯ-РАЗРЕШЕННЫХ И ПОЛЯРИЗАЦИОННО-РАЗРЕШЕННЫХ СПЕКТРОВ ЛАЗЕРНО-ЭМИССИОННОЙ ПЛАЗМЫ АЛЮМИНИЕВОГО СПЛАВА

G. A. Wubetu [1,2*], J. T. Costello [3], T. J. Kelly [4], P. Wachulak [5], A. Bartnik [5], W. Skrzeczanowski [5], H. Fiedorowicz [5]

УДК 543.423:533.9

[1] Колледж естественных наук Университета Бахир Дар, Бахир Дар, Эфиопия; e-mail: getasew.wubetu2@mail.dcu.ie, getasew.admasu@bdu.edu.et
[2] Колледж естественных и вычислительных наук Аддис-Абебского университета, Аддис-Абеба, Эфиопия
[3] Национальный центр плазменной науки и технологии (NCPST) и школа физических наук Дублинского городского университета, Гласневин, Дублин, Ирландия
[4] Атлантический технологический университет, Голуэй, Ирландия
[5] Институт оптоэлектроники, Военный технологический университет (MUT), Варшава, Польша

(Поступила 21 января 2022)

Методами оптической эмиссионной спектроскопии с временным (LIBS) и поляризационным разрешением (PRLIBS) исследована лазерная плазма, сформированная на сплавах алюминия, в видимой области в воздушной атмосфере при давлении 10^{-4} мбар. Спектральное отношение сигнал-фон значительно увеличивается для PRLIBS по сравнению с LIBS для линии излучения 415 нм Mn, присут-

**Full text is published in JAS V. 90, No. 1 (http://springer.com/journal/10812) and in electronic version of ZhPS V. 90, No. 1 (http://www.elibrary.ru/title_about.asp?id=7318; sales@elibrary.ru).

ствующего в образце в следовой концентрации. Результаты интерпретированы в рамках излучательно-рекомбинирующей плазмы, в которой свободные электроны захватываются ионами для излучения. Степень поляризации для матричных линий Al^0 (396.15 нм) и Al^{2+} (569.6 нм) определяется количественно с использованием соседних неполяризованных линий излучения. Параметры плазмы измеряются и сравниваются со степенью поляризации для определения доминирующего механизма поляризованного излучения. Показано, что PRLIBS является полезным и простым дополнением, способным улучшить экспериментальную производительность LIBS.

Ключевые слова: *лазерно-искровая эмиссионная спектроскопия, лазерно-искровая эмиссионная спектроскопия с поляризационным разрешением, отношение сигнал-фон, предел обнаружения, излучательная рекомбинация.*

Introduction. Laser-induced breakdown spectroscopy (LIBS) is a widely used analytical technique for the characterisation of materials, especially their elemental composition [1–4]. Focusing a pulsed laser onto a solid target, a hot plume of material is formed that emits radiation comprising both broadband continuum and line emission from its constituent ions and atoms. The key LIBS parameter is the limit of detection (LoD), which depends strongly on the signal-to-background ratio (SBR) [1, 4]. Polarization-resolved laser-induced plasma spectroscopy (PRLIBS) is a potentially promising alternative to normal LIBS [5–7]. The addition of polarization state selection, by placing a polariser in front of the entrance slit of the LIBS spectrometer, is a simple way of potentially reducing the background continuum emission, thereby increasing SBR and improving LoD [6]. In a laser-produced plasma, anisotropies in the polarization of emitted radiation can occur [8–13]. Previous studies tend to focus their investigations on either the discrete line emission [5] or the broadband emission [6, 7]. The early-stage plasma emission spectrum is typically dominated by continuum radiation as a result of radiative recombination of electrons and ions (free-bound electron transition) and also inverse bremsstrahlung (free-free transitions) [8, 9]. The line radiation is the result of excited state relaxation in bound-to-bound transitions within excited atoms and ions [8, 9]. However, these studies focussed on wider spectroscopic windows and very little was reported on the mechanisms that lead to anisotropies in the line emission from plasmas. The nature of anisotropy in continuum emission polarization is attributed to asymmetry in the electron velocity distribution function (EVDF), which is usually reduced to a bi-Maxwellian distribution for the free electrons in the plasma plume [10, 11]. The line emission polarization arises from a non-uniform population of the magnetic sublevels, which are excited by a laser field [5]. The anisotropy in the polarization of continuum emission arises from the existence of fast and slow EVDF components [5, 7]. It has been postulated that this can in turn transfer to line emission as bound excited states populated in the electron-ion recombination step decay to lower bound states [14].

In this study we present the results of a PRLIBS study on an aluminium alloy using optical emission spectroscopy. Specifically, we measure the degree of polarization of two spectral emission lines from the bulk aluminium (neutral Al at a wavelength of 394.15 nm and doubly charged Al at a wavelength of 596.2 nm) and a spectral emission line that arises from low-concentration Mn presenting in the alloy (at a wavelength of 415 nm). SBR was measured for all three spectral lines in the PRLIBS regime and compared with the polarization-unresolved (normal LIBS) case. In each case, an enhanced SBR was obtained for both bulk sample and trace elements.

Experimental setup. Figure 1 shows the time-resolved PRLIBS setup to track the evolution of the plasma with time. A BRIO^{TM} Nd:YAG laser, operating at 1064 nm, was used to ablate the target, with a laser fluence of 223 J/cm^2 (corresponding to an irradiance of 5.6×10^{10} W/cm^2) with a pulse duration of 4 ns and operated with a pulse repetition rate (PRF) of 20 Hz. The intensity of the laser was varied using a combination of a half-wave plate and a polariser. A well-calibrated energy meter was used before and after each measurement to ensure the correct reading of the laser pulse energy. For this experiment, the laser was focused normal to the target, using a planoconvex lens (f = 100 mm), onto an Al alloy target to produce the plasmas. The target was mounted on a remotely controlled x-y-z translation stage with micron-scale resolution in a sealed vacuum chamber at a background air pressure of 10^{-4} mbar. This ensured that a fresh target spot could be revealed after each laser pulse. Each spectrum was measured three times: first with a dichroic polariser set at 0°; then with a dichroic polariser set at 90° in front of the spectrometer and finally without a polariser. 0° represents the direction parallel to the target normal, and 90° is the perpendicular direction. The degree of polarization can be determined by taking the difference between the two polarization measurements

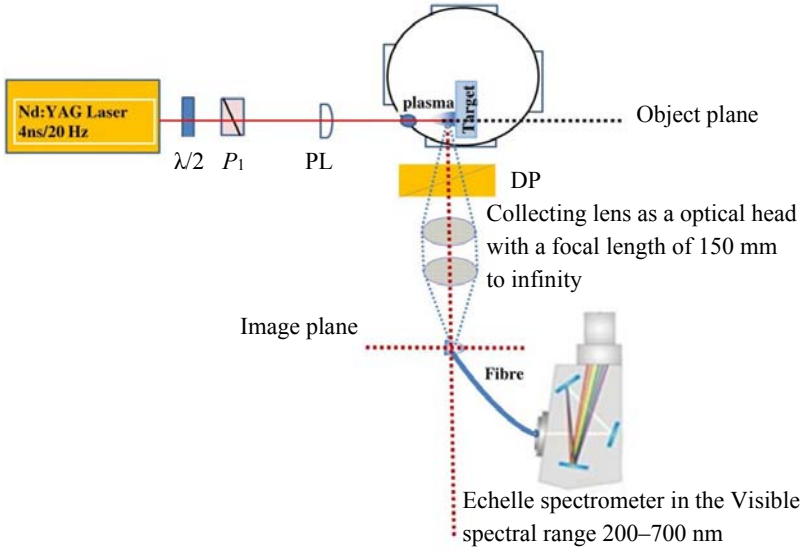

Fig. 1. Schematic diagram of the PRLIBS system (λ/2, half-wave plate; P_1, polariser; PL, plano-convex lens; DP, dichroic polariser).

dividing by the sum. However, the use of a dichroic polariser requires taking a laser shot for each polarization state separately; thus, the repeatability of the measurement was limited by shot-to-shot fluctuations. To reduce the impact of shot-to-shot fluctuations, ten spectra were averaged for each pulse energy used. The light emitted was imaged normal to the laser propagation axis by a C52 ANDOR™ optical head (with a focal length of f = 150 mm) and then focused on to a 2-m-long fused silica fibre, with a core diameter of 50 μm, connected to an Echelle ESA™ 4000 spectrometer (LLA GmbH, Berlin, Germany) equipped with an ICCD detector (Kodak™ KAF 1001 camera). The spectrometer operated within the wavelength range 200–700 nm with a mean spectral resolution of $\lambda/\Delta\lambda \approx 20{,}000$. An OG3 Al alloy (from OML™ SKAWINA) in the form of a circular disc was used as a target for the experiments. The concentrations of aluminium and other trace metals in this alloy are (w/w%): Cu = 4.3, Mg = 0.34, Ti = 0.18, Fe = 0.29, Si = 0.27, Zn = 0.20, Mn = 0.08, Ni = 0.04, and Al = 94.3.

The measurements were performed at an ICCD gate width of 500 ns and a time delay, with respect to the laser pulse, of 50 ns. In this experiment, we compared spectra without a polariser in place (called LIBS spectra) with spectra where the polariser is placed in front of the spectrometer (called PRLIBS spectra). The degree of polarization is found by:

$$P_\lambda = \frac{I_H - I_V}{I_H + I_V}, \tag{1}$$

where I_H is the intensity of the light polarised parallel to the incident laser propagation axis and I_V is the intensity of the light polarised perpendicular to the incident laser propagation axis.

Results and discussion. *Emission from laser-produced plasmas.* Figure 2 displays the average of ten single-shot, time-resolved optical emission spectra from an Al alloy plasma produced by a laser pulse energy of 70±3 mJ (corresponding to a fluence of 223±10 J/cm^2) at a background pressure of 10^{-4} mbar within the visible spectral range. The plasma emission was taken from a region located 1 mm away from the target surface at a gate width of 500 ns and a time delay of 50 ns with respect to the laser pulse. Both LIBS and PRLIBS spectra, covering the wavelength range of 380–600 nm (Fig. 2). Each spectrum comprises Al^{2+}, Al^{+}, and Al^{0} lines superimposed on a broadband continuum. The dominant lines observed are Al^{0} 394.4 nm, Al^{0} 396.15 nm, Al^{2+} 452.9 nm, Al^{+} 466.3 nm, Al^{+} 559.33 nm, Al^{2+} 569.6 nm, and Al^{2+} 572.3 nm. The corresponding spectroscopic parameters and electronic transitions of the ionic and neutral line emissions are given in Table 1. The assignments were made using the data taken from the NIST database [15].

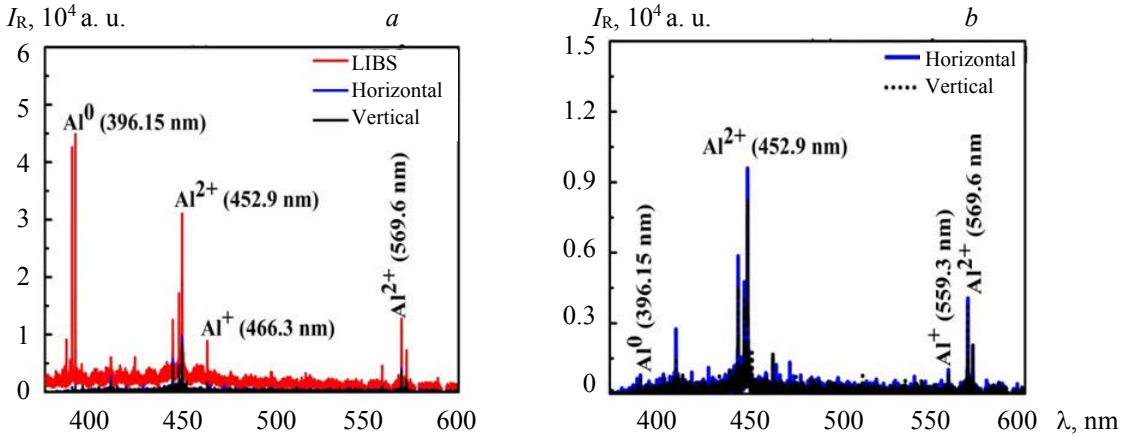

Fig. 2. The LIBS (a) and PRLIBS (b) spectra of an Al alloy (OG3) for a laser pulse energy of 70 mJ at a background pressure of 10^{-4} mbar. The laser fluence was 223 J/cm^2 with an ICCD camera gate width of 500 ns and a time delay of 50 ns.

TABLE 1. Spectroscopic Parameters for Al^0 (at 394.4 and 396.15 nm), Al$^+$ (at 466.3 and 559.33 nm), and Al^{2+} (at 569.6 and 572.3 nm) and Mn (415 nm) with Assignments from the NIST Database

Wavelength, nm	Transition	g_kA_{ki} ×10^8, 1/s	E, eV
Al^0 394.4, 396.15	$4s(^2S_{1/2})\rightarrow 3p(^2P^0_{1/2,3/2})$	1.2	3.14
Al^{2+} 414.99	$3p^65f(^2P^o_{7/2})\rightarrow 2p^64d(^1D_2)$	16.4	23.54
Al$^+$ 466.3	$3s4p(^1P^o_1)\rightarrow 3p^2(^1D_2)$	1.74	13.26
Al^{2+} 452.9	$2p^64d(^2P_{5/2})\rightarrow 2p^64p(^2P^o_{3/2})$	14.9	20.55
Al$^+$ 458.97	$3s7f(^3F^o_4)\rightarrow 3s4d(^3D_3)$	0.078	17.765
Al$^+$ 559.33	$3s4d^1D_2\rightarrow 4s4p^1P^o_1$	4.63	15.47
Al^{2+} 569.6, 572.3	$4p(^2P^o_{3/2,1/2})\rightarrow 4s(^2S_{1/2})$	3.51, 1.73	17.82
Mn$^+$ 415 nm	$3d\,^5(^4F)4s4p(^3P^o)(^6G^o_{7/2})\rightarrow 3d\,^6(^3G)4sb(^4G_{9/2})$	19	7.65

N o t e. g_kA_{ki} is the product of transition probability and statistical weight and E is the upper state energy.

Polarization-resolved spectra. Figure 3 shows a comparison of LIBS and PRLIBS spectra where the Al^0 (394.4 and 396.15 nm) and Al^{2+} (569.6 and 572 nm) lines are shown in greater detail. It is known [8, 12, 13] that the 394.4 and 572.3 nm lines are unpolarised. The normalised degree of polarization of the 396.15 nm wavelength line is given by Eq. (1):

$$P_\lambda = \frac{\dfrac{\sum I_H^{396.15\text{nm}}}{\sum I_H^{394.4\text{nm}}} - \dfrac{\sum I_V^{396.15\text{nm}}}{\sum I_V^{394.4\text{nm}}}}{\dfrac{\sum I_H^{396.15\text{nm}}}{\sum I_H^{394.4\text{nm}}} + \dfrac{\sum I_V^{396.15\text{nm}}}{\sum I_V^{394.4\text{nm}}}}. \qquad (2)$$

The degrees of polarization obtained using Eq. (2) were −0.07±0.02 for the Al 396.15 nm neutral line and 0.10±0.03 for the Al^{2+} 569.6 nm line. The negative sign for the 396.15-nm line is due to its being a 4*s*–3*p* (*s*–*p*) transition whereas for the 569.6-nm line the sign is positive as it is due to a 4*p*–4*s* (*p*–*s*) transition (Table 1).

The time- and polarization-resolved spectra of Al^{2+} show the 569.6 and 572.3 nm lines, corresponding to the transitions $4p(^2P^0_{3/2})\rightarrow 4s(^2S_{1/2})$ and $4p(^2P^0_{1/2})\rightarrow 4s(^2S_{1/2})$, respectively, at a background pressure of 10^{-4} mbar. They are shown in Fig. 3b. The blue colour in the graph illustrates the spectra of parallel (horizontal) and the black colour perpendicular (vertical) polarization (wrt. the spectrometer slit orientation) at a gate width of 500 ns and a gate delay of 50 ns from the plasma formation. The degree of polarization (P) of the 396.15- and 569.6-nm lines can be calculated using Eq. (2) with the 394.4 and 572.3 nm lines for the calibration of the grating for both the horizontal and the vertical polarization states. This is because the selection rule from quantum mechanics ensures that the lines at 394.4 and 572.3 nm are unpolarised. Sharma and

Thareja [16] tracked the time and polarization emission from a laser-produced plasma of aluminium in a nitrogen ambient gas and in vacuo. They found that P is almost constant for a lower laser pulse energy of 44 mJ (corresponding to a fluence of 89 J/cm^2) and oscillates with delay time at a higher laser pulse energy of 256 mJ (corresponding to a fluence of 842 J/cm^2) using 6-ns pulse width Nd:YAG laser at the fundamental wavelength of 1064 nm.

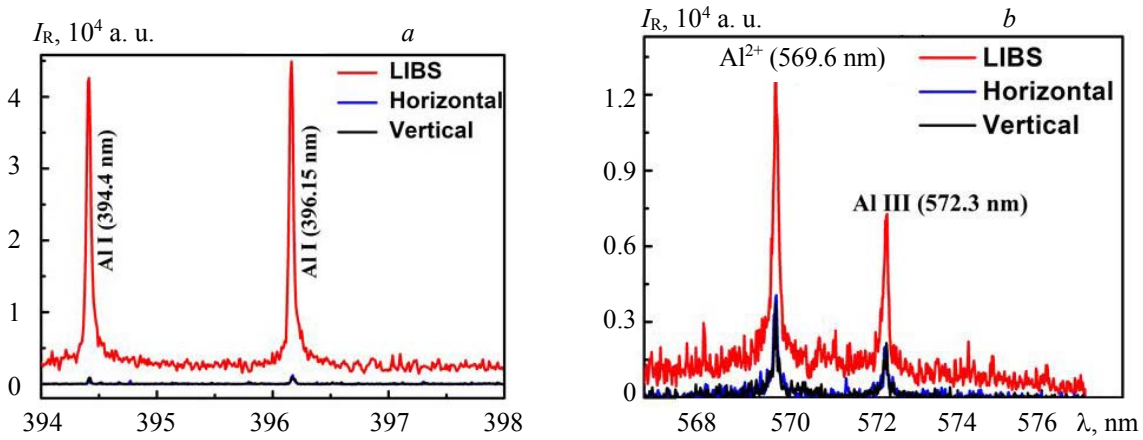

Fig. 3. Comparison of the LIBS and PRLIBS spectra produced at a laser pulse energy of 70 mJ. The spectra were taken at a time window of 500 ns and a delay of 50 ns, Al^0 at 396.15 nm (a), and Al^{2+} at 569.6 nm (b).

Figure 4 shows a comparison of the trace element of the LIBS and PRLIBS spectrum of Mn I 415 nm. From Eq. (1), the degree of polarization obtained for this matrix was 0.160±0.003. For both spectra, Voigt profiles with a spectral resolution of 0.29, 0.023, and 0.059 nm provided good fits to the highlighted lines. The integrated area under these Voigt profiles was then used to find the intensity of a particular spectral line.

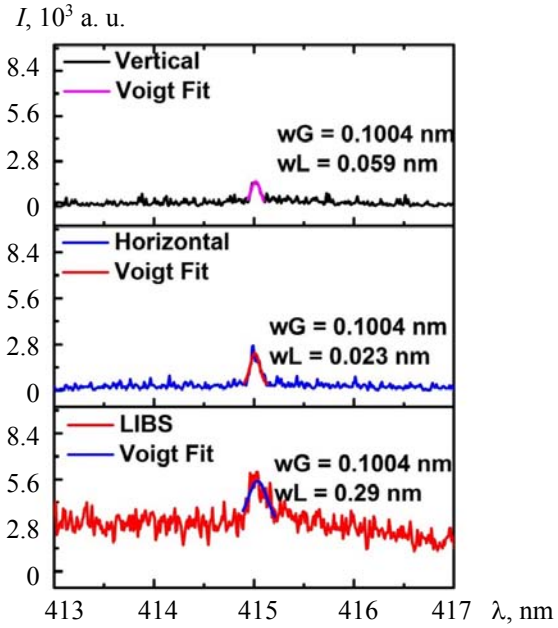

Fig. 4. Comparison of the LIBS and PRLIBS spectra of Mn I 415 nm produced at a laser pulse energy of 70 mJ. The spectra were taken at a time window of 500 ns and a delay of 50 ns.

Partial Grotrian diagrams for Al I, Al II, and Al III lines of interest. Figure 5 displays a partial energy level diagram for atomic aluminium showing the fine and magnetic sublevel splitting for the line Al^0 396.15 nm corresponding to the transition $3s^24s(^2S_{1/2})\rightarrow 3s^23p(2P^0{}_{3/2})$ and 394.4 nm corresponding to the transition $3s^24s(^2S_{1/2})\rightarrow 3s^23p(^2P^0{}_{1/2})$, respectively.

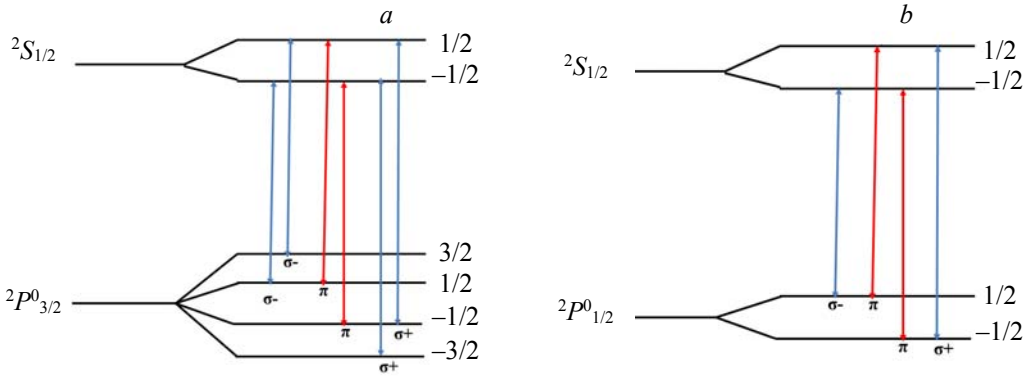

Fig. 5. Energy level splitting for the atomic Al transitions at (a) 396.15 nm ($3s^24s^2S_{1/2}\rightarrow 3s^23p^2P^\circ{}_{3/2}$) and (b) 394.4 nm ($3s^24s^2S^0{}_{1/2}\rightarrow 3s^23p^2P^0{}_{1/2}$).

In transitions between the above levels, when the change of magnetic quantum number is zero, i.e., $\Delta m = 0$, the light is linearly polarised and represented as π polarization. However, when the magnetic quantum number changes by unity, i.e., $\Delta m = \pm 1$, the light is right circularly or left circularly polarised, which is represented by ±σ. The 394.4 nm line is unpolarised with four multiplets having two σ and two π-polarization transitions [2]. Consequently, the net degree of polarization (P) is zero owing to the equal strength of the counter-rotating polarization states. However, the 396.15 nm line is polarised because of the difference in the strength of four σ and two π-polarised transitions. Thus, the net degree of P is different from zero owing to unequal strength in these counter-rotating polarizations. The unpolarised 394.4-nm line is used in conjunction with the 396.15-nm polarised line to calibrate the spectrometer for polarization state sensitivity.

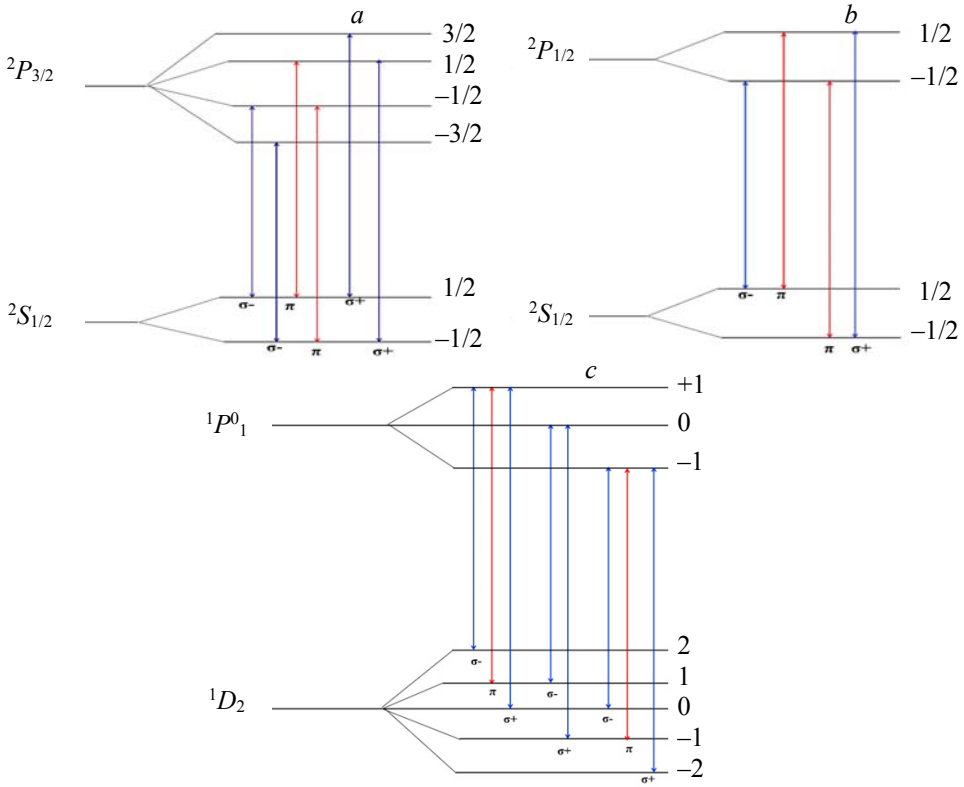

Fig. 6. Magnetic sublevel structure for the (a) 569.6 nm, (b) 572.3 nm, and (c) 466.3 nm lines.

Figure 6 displays the energy level diagrams for the Al^{2+} transitions $4p(^2P^0_{3/2})\rightarrow 4s(^2S_{1/2})$ at 569.6 nm, $4p(^2P^0_{1/2})\rightarrow 4s(^2S_{1/2})$ at 572.3 nm and the Al^+ transition $3s4p(^1P^0_1)\rightarrow 3p^2(^1D_2)$ at 466.3 nm, respectively. The magnetic sublevel structures for the transitions of interest are shown. The 572.3-nm line (Fig. 6b) is unpolarised and thus can be used to calibrate the polarised neighbouring 569.6-nm line. Kim et al. [12] and Sharma and Thareja [8] used the 572.3 nm line for polarization sensitivity calibration for the Al^{2+} doublet. The discrete lines become polarised in the plasma owing to a non-statistical distribution of the atomic and ionic population amongst magnetic sublevels in selected parts of the plasma where there is an anisotropy in EVDF [17].

Comparison of SBR. Here, SBR for two Al matrix lines, namely Al^0 (396.15 nm) and Al^{2+} (569.6 nm) lines, and the minor (trace) element Mn (415 nm) line are compared for the LIBS and PRLIBS spectra. Farid et al. [9] reported SBR using the peak intensity of the signal and the average intensity of the background. However, in our study, in order to minimise any errors due to instrumental line broadening, the area under the line profile was used as a measure of the signal intensity (S) and the summation of the background intensity over the same spectral width (number of pixels) was used as a measure of the associated background (B), to extract SBR. The equation for SBR is given by:

$$\text{SBR} = (\sum I_{\text{sig}} - \sum I_{\text{backgr}})/\sum I_{\text{backgr}}, \tag{3}$$

where $\sum I_{\text{sig}}$ is the integrated intensity of the line and $\sum I_{\text{backgr}}$ is the integrated intensity of the background. Table 2 shows the signal and background counts for each line measured. Table 3 shows SBR extracted from both LIBS and PRLIBS spectra. A significant increase in SBR for the trace element Mn on the 415-nm line is evident, as shown in Table 3.

TABLE 2. LIBS and PRLIBS Total Line Intensities (Counts) Obtained by Determining the Area Under Each Spectral Line along with Corresponding Background Intensities

Spectrum	LIBS	Horizontal PRLIBS	Vertical PRLIBS
Al^0 (396.15 nm)	298998	2568	2058
Background	51353	222	183
Al^{2+} (569.6 nm)	211208	49182	20334
Background	138838	39216	22953
Mn I (415 nm)	145539	32664	23535
Background	97293	10560	10541

TABLE 3. The SBR of the LIBS and PRLIBS spectra

Spectrum	Al^0 (396.15 nm)	Al^{2+} (569.6 nm)	Mn^+ (415 nm)
LIBS	4.82	0.52	0.5
Horizontal PRLIBS	10.6	1.42	2.1
Vertical PRLIBS	10.2	0.7	1.23

Plasma diagnostics. The plasma electron density and temperature were measured using spectroscopic methods, namely, the stark broadening and line ratio methods. An isolated line of Al^+ (at 466.3 nm) was used to estimate the electron density. This line is broadened by the Stark effect. The full width half maximum (FWHM) of the Stark broadened line is given by [18]:

$$\Delta\lambda_{\text{stark}} = 2wn_e/10^{16} + 3.5A\frac{(n_e)}{10^{16}}^{1/4} + \left[1 - BN_D^{-1/3}\right]wn_e/10^{16}. \tag{4}$$

In the case of dense laser-produced plasmas, the Stark effect is dominated by electron collisions with the atomic constituents of the plasma plume, which are represented by the first term in Eq. (4). Hence, the second and third terms can be neglected and so, to a very good approximation, the linewidth for an isolated line is given by [18]:

$$\Delta\lambda_{1/2} \approx 2wn_e/10^{16}, \tag{5}$$

where $\Delta\lambda_{1/2}$ is the Stark width, w = 0.0615 nm (half width) is the electron impact parameter for Al^+ at a wavelength of a 466.3 nm line for a temperature of 10,000 K [19] and n_e is the electron density, respectively. Figure 3 shows LIBS and PRLIBS spectra of the OG3 sample plasmas with the Al^+ line visible at a wavelength of 466.3 nm in each case.

Figure 7 shows the spectral lines of LIBS and PRLIBS (vertical polarization). The spectral lines were fitted using a Voigt profile, which is the convolution of Gaussian and the Lorentzian profiles. Here the former represents the instrument function of the spectrometer, i.e., the spectral broadening introduced by the spectrometer and has a value of 0.02 nm FWHM. The Lorentzian component of the profile, which represents the Stark broadening contribution to the line profile, was used to estimate the electron density in this study. The natural broadening is negligible. The electron densities were estimated to be 1.7×10^{16} cm^{-3} for LIBS and 0.7×10^{16} cm^{-3} for the vertical PRLIBS spectra. This indicates that the vertical line emission comes from a lower density region of the plasma compared with the horizontal line emission. This measurement is in line with our measurement of the degree of polarization that indicated that the horizontal line emission intensity was greater than that obtained from the vertically polarised component.

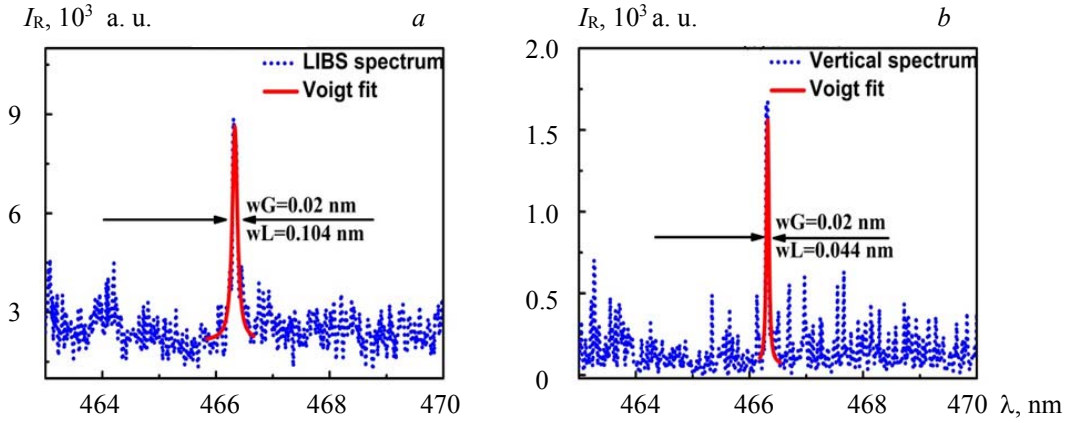

Fig. 7. Voigt fits for (a) LIBS and (b) PRLIBS spectra showing Al^+ 466.3 nm for a time delay of 50 ns at a background pressure of 1×10^{-4} mbar. The laser fluence was 223 J cm^{-2} with an ICCD camera gate width of 500 ns.

Assuming local thermodynamics (LTE), the temperature can be calculated from the intensity ratio of the pair of spectral lines that originate from different ion stages of the same element. The intensity ratio is related to the basic atomic parameters by the equation [18]:

$$I_1 / I_2 = \left(\frac{A_1\lambda_2 g_1}{A_2\lambda_1 g_2}\right)\exp\left(-\frac{E_1 - E_2}{k_B T_e}\right), \tag{6}$$

where I_1 and I_2 are the relative intensities of the emitted lines, A_1 and A_2 are the corresponding transition rates, in s^{-1}, g_1 and g_2 are the statistical weights of the levels of the transitions involved, i.e. $(2J+1)$, where J is the total angular momentum, and E_1 and E_2 are the energies of those states. The electron temperature can be determined using the line ratio:

$$\ln\left(I_1 / I_2\right) = \ln\left(\frac{A_1 g_1 \lambda_2}{A_2 g_2 \lambda_1}\right) - \left(\frac{E_1 - E_2}{k_B T_e}\right). \tag{7}$$

The intensity ratio from the Al^+ line at a wavelength of 559.33 nm and the Al^{2+} line at a wavelength of 569.6 nm was used to quantify the plasma temperature from the LIBS and PRLIBS spectra. The intensity values (in counts), obtained by taking the area under the profile of each of these lines, are given in Table 4.

TABLE 4. LIBS Along with Horizontal and Vertical PRLIBS Total Line Intensities (in ICCD counts) Obtained by Determining the Area under Each Spectral Line

Spectral lines and associated wavelengths	LIBS	PRLIBS	
		horizontal	vertical
Al^+ (559.33 nm)	31144	5746	5564
Al^{2+} (569.6 nm)	211208	49182	39216

Using Table 2 and substituting into Eq. (6) the plasma temperature obtained from only the LIBS spectrum was determined to be 1.1±0.3 eV. The temperatures obtained from the horizontal and vertical PRLIBS spectra were 1.0±0.4 and 1.05±0.25 eV, respectively.

In order to check the validity of the assumption that LTE pertained in the plasma, the McWhirter criterion [20, 21] was used. This equation is given by:

$$n_e \geq 1.6 \times 10^{12} T_e^{1/2} \left(E_1 - E_2\right)^3, \quad (8)$$

where n_e is the electron density, T_e is the electron temperature, E_1 is the upper state energy of the Al^+ transition giving rise to the line at a wavelength of 559.33 nm and E_2 is the upper state energy of the Al^{2+} transition corresponding to a wavelength of 569.6 nm. Using Eq. (8) n_e is estimated to be 2.9×10^{15} cm^{-3}, which is less than the electron density obtained experimentally. Consequently, the McWhirter criterion is satisfied and the assumption of LTE to estimate plasma parameters [20, 21] is valid for each polarization state (horizontal and vertical polarization) [13].

Based on Kim and Kim's [12] interpretation and the Saha equation, the calculated low density and temperature indicated that the upper states could be populated by radiative recombination of Al^+ for the neutral emission (at 396.15 nm) and Al^{3+} for the double ionic emission (at 569.6 nm) to the electrons. These upper state populations could then create a population imbalance and lead to the emission of lines with a non-zero degree of polarization [17]. As the density and the temperature are so low, the radiative interactions are dominant over collisional interactions and are therefore likely to be the underlying driver of anisotropic emission [12, 13].

The observed difference in SBR when comparing LIBS and PRLIBS indicates that the continuum broadband radiation is also polarised. The polarization of this emission is explained by viewing this plasma as being out of equilibrium and dominated by recombination effects. The recombination of an electron by a highly charged ion to produce a lower charged ion results in the release of broadband emission, which is polarised owing to the bi-Maxwellian nature of the plume. The subsequent line emission is produced as the excited ion then further decays to the ground state. As a result of the plasma recombining out of equilibrium, the resulting line emission is also polarised [12, 13, 16].

Our results also indicate that these polarization effects affect the trace element Mn (at 415 nm) as well as the bulk aluminium. Therefore, under our experimental conditions, we can say that PRLIBS is a viable method with which SBR, and therefore the limit of detection of low-concentration materials in a bulk alloy are improved. For the Al^0 emission, we see an improvement of SBR of ~2.5 for PRLIBS, compared with LIBS. For the low-concentration Mn emission, we see similar behaviour when averaged between vertical and horizontal polarization states. We are careful to note that, owing to the dynamic nature of the plasma parameters, we can only attest to the benefits of PRLIBS under our experimental conditions. However, owing to the relative ease of the experimental setup, the relatively high precision of the method, and the high degree of control over the setup, we do suggest that it is a useful addition to a LIBS setup that can be tuned when optimising the signal along with other experimental parameters (distance from the target, gate time, gate width, laser fluence, etc.) as it could lead to benefits.

Conclusions. A polarization-resolved spectroscopic LIBS measurement was performed in an Al alloy using an Echelle spectrometer. We found that the emission was dominated by the Al^0 emission but that there was measurable emission from the low concentration Mn species present in the alloy. Both the Al and Mn signals were found to be partially polarised with degrees of polarization of –0.07±0.02 for the Al neutral emission and 0.160±0.003 for the Mn emission. Plasma diagnostic measurements of temperature and density revealed that the plasma is likely to be in a recombining state which explains the partial polarization of the emission being driven from an anisotropic recombining plasma leading to a statistical imbalance in the magnetic sub-levels of the upper states. We found that the SBR is clearly improved for both the Al emission lines and the emission of Mn. The improvement was found to be close to 2 for both. Therefore, we conclude that this experimental setup can be used to enhance the performance of LIBS instruments.

Acknowledgments. The work is supported by the Education, Audio-Visual and Culture Executive Agency (EACEA) Erasmus Mundus Joint Doctorate Programme EXTATIC (Project No. 2012-0033), Science Foundation Ireland (Grants Nos. 16/RI/3696 and 19/FFP/6956), and the Sustainable Energy Authority of Ireland (SEAI) (Grant No. 19/RDD/556). The work is associated with COST Action CA17126. TJK wishes to acknowledge support from the GMIT PIRATE project.

REFERENCES

1. N. Hans, D. W. Omenetto, *Appl. Spectrosc*., **64**, 335A (2010).
2. N. Lucas, *The Application of Laser Induced Breakdown Spectroscopy (LIBS) to the Analysis of Geological Samples in Simulated Extra-Terrestrial Atmospheric Environments*, PhD Thesis, Institute for Materials Research, University of Salford, Salford, UK (2007).
3. F. Anabitarte, A. Cobo, J. M. Lopez-Higuera, *ISRN Spectrosc.*, **1** (2012).
4. M. A. Khater, *Opt. Spectrosc*., **115**, 574 (2013).
5. A. Eslami Majd, A. S. Arabanian, R. Massudi, *Opt. Lasers Eng*., **48**, 750 (2010).
6. Y. Zhao, S. Singha, Y. Liu, R. J. Gordon, *Opt. Lett*., **34**, 494 (2009).
7. H. M. Milchberg, J. C. Weisheit, *Phys. Rev. A*, **26**, 1023 (1982).
8. A. K. Sharma, R. K. Thareja, *Appl. Surf. Sci*., **253**, 3113 (2007).
9. N. Farid, S. S. Harilal, H. Ding, A. Hassanein, *J. Appl. Phys*., **115**, 1 (2014).
10. J. C. Kieffer, J. P. Matte, M. Chaker, Y. Beaudoin, C. Y. Chien, S. Coe, G. Mourou, J. Dubau, M. K. Inal, *Phys. Rev. E*, **48**, 4648 (1993).
11. M. E. Asgill, H. Y. Moon, N. Omenetto, D. W. Hahn, *Spectrochim. Acta B: At. Spectrosc*., **65**, 1033 (2010).
12. J. Kim, D. E. Kim, *Phys. Rev. E - Stat. Nonlinear, Soft Matter Phys*., **66**, 1 (2002).
13. G. A. Wubetu, H. Fiedorowicz, J. T. Costello, T. J. Kelly, *Phys. Plasmas*, **24**, 013105 (2017).
14. G. A. Wubetu, T. J. Kelly, P. Hayden, H. Fiedorowicz, W. Skrzeczanowski, J. T. Costello, *J. Phys. B At. Mol. Opt. Phys*., **53**, 065701 (2020).
15. https://physics.nist.gov/PhysRefData/ASD/lines_form.html.
16. A. K. Sharma, R. K. Thareja, *J. Appl. Phys*., **98**, 033304 (2005).
17. J. S. Penczak, Y. Liu, R. J. Gordon, *Opt. Lett*., **34**, 494 (2009).
18. J. P. Singh, S. N. Thanku, *Laser Induced Breakdown Spectroscopy*, Elsevier (2007).
19. A. W. Allen, M. Blaha, W. W. Jones, A. Sanchez, H. R. Griem, *Phys. Rev. A*, **11**, 477 (1975).
20. J. Dardis, *Interactions Of Intense Optical and Extreme-Ultraviolet Lasers with Atoms and Solids*, PhD Thesis, Dublin City University (2009).
21. C. Fallon, *Optical Diagnostics of Colliding Laser Produced Plasmas: Towards Next Generation Plasma Light Sources*, PhD Thesis, Dublin City University (2013).